Journal of Nano- and Electronic Physics
Vol. **14** No 4, 04017(6pp) (2022)

Журнал нано- та електронної фізики
Том **14** № 4, 04017(6cc) (2022)

Optical Characterization of $CdSe_{1-x}Te_x$ Nanocrystals Grown in Borosilicate Glass

Y.M. Azhniuk[1,2], A.V. Gomonnai[1,2], Yu.I. Hutych[1], V.V. Lopushansky[1], D.R.T. Zahn[3]

[1] *Institute of Electron Physics, NAS of Ukraine, 21, Universytetska St., 88017 Uzhhorod, Ukraine*
[2] *Uzhhorod National University, 46, Pidhirna St., 88000 Uzhhorod, Ukraine*
[3] *Semiconductor Physics, Chemnitz University of Technology, D-09107, Chemnitz, Germany*

(Received 12 April 2022; revised manuscript received 08 August 2022; published online 25 August 2022)

$CdSe_{1-x}Te_x$ nanocrystals (NCs) were obtained by diffusion-limited growth in borosilicate glass and studied by optical absorption, photoluminescence (PL), and Raman spectroscopy. Several Raman-based approaches to determine the NC chemical composition were analyzed. Based on the Raman data, it is shown that for $CdSe_{1-x}Te_x$ NCs with intermediate x ($0.4 < x < 0.6$) the Te content slightly decreases with the thermal treatment temperature and duration. Confinement-related maxima in the optical absorption spectra of glass-embedded $CdSe_{1-x}Te_x$ NCs enable their average size to be estimated, while their smeared appearance reveals a noticeable size dispersion. A rather narrow near-bandgap PL peak with a small Stokes shift dominates in the PL spectra of glass-embedded $CdSe_{1-x}Te_x$ NCs, while a lower-energy surface-mediated PL band appears only as a shoulder and vanishes with increasing Te content.

Keywords: Nanocrystals, Diffusion-limited growth, Photoluminescence, Raman spectroscopy.

DOI: 10.21272/jnep.14(4).04017 PACS number: 78.67.Bf

1. INTRODUCTION

Within recent decades, colloidal synthesis techniques have been developed to produce high-quality semiconductor nanocrystals (NCs) with tunable size and narrow size dispersion [1]. Still, in some cases application purposes require semiconductor NCs to be embedded in a robust transparent matrix. This can be achieved by the well-known technique of diffusion-limited growth in silicate glass matrices, widely used to obtain glass-embedded CdS and CdSe NCs, as well as related solid solution NCs [2, 3]. Meanwhile, fabrication of tellurium-containing NCs, in particular ternary $CdSe_{1-x}Te_x$, by this technique is less known, although such NCs in a stable environment can be interesting for applications. In most cases, measurements were performed for a limited set of samples in a rather narrow compositional and size interval [4-7].

Various techniques were employed for the characterization of glass-embedded telluride-based ternary II-VI semiconductor NCs, including transmission electron microscopy [5], X-ray diffraction [5], Raman scattering [4, 6], optical absorption [5, 7], photoluminescence [5], and ultrafast pump-and-probe spectroscopy [7]. Here we report on glass-embedded ternary $CdSe_{1-x}Te_x$ NCs studied by optical absorption, photoluminescence (PL), and Raman spectroscopy.

2. EXPERIMENTAL

$CdSe_{1-x}Te_x$ NCs were obtained by diffusion-limited growth in SiO_2-B_2O_3-Na_2O-K_2O borosilicate glass from a supersaturated solution basically similar to the technique described earlier [2, 3]. Commercial Schott glasses containing $CdSe_{1-x}Te_x$ and $CdS_{1-x}Se_x$ NCs were used as initial materials. They were heated above 1000 °C for 1 h, when the existing II-VI NCs were dissolved and a colorless transparent glass with randomly dispersed cadmium and chalcogen atoms was produced. Pieces of this glass were subjected to thermal treatment with duration τ from 2 to 12 h, the temperature T_a was in the range from 600 to 700 °C. After rapid cooling down to room temperature they were polished, and their optical properties were studied.

Optical absorption spectra of glass-embedded NCs were measured using a LOMO MDR-23 spectrometer. For PL measurements, a Horiba LabRAM spectrometer and a solid-state laser (514.7 nm) were used. Raman spectra were measured using a Dilor XY 800 spectrometer or a Horiba LabRAM spectrometer with a cooled CCD camera, the excitation was provided by a solid-state (514.7 nm), a He-Ne (632.8 nm), or a Kr^+ (647.1 and 676.4 nm) laser. All measurements were performed at room temperature. In some cases, the Raman spectra were observed against a broad background of a PL signal which was subsequently subtracted for the analysis of the Raman spectra.

3. RESULTS AND DISCUSSION

Raman spectra of $CdSe_{1-x}Te_x$ NCs embedded in borosilicate glass are shown in Fig. 1. Since the NCs comprise only a quite small (below 1 %) fraction of the sample scattering volume, it is essentially important to select the Raman excitation wavelength providing resonant enhancement of the LO phonon peaks. Hence, in most cases in the Raman spectra of II-VI NCs dispersed in dielectric media only LO phonons are revealed [8 and references therein]. Similarly to much more extensively studied $CdS_{1-x}Se_x$ NCs [9, 10], $CdSe_{1-x}Te_x$ NCs reveal a two-mode compositional behavior of their phonon spectra with CdTe-related LO_1 and CdSe-related LO_2 phonon peaks [6]. The frequency difference of these two peaks is a good measure of the chemical composition of the NCs and (especially in the case they are embedded in a dielectric matrix) Raman spectroscopy is the most convenient, fast, and non-destructive technique to evaluate the NC composition [8]. Based on the experimental data for $CdSe_{1-x}Te_x$ NCs which were compared to Raman and infrared data for the corresponding bulk crystals [6 and references therein], the compositional dependences of the LO phonon frequen-

cies and their difference were built enabling the ternary NC composition to be determined. These dependences, as for $CdS_{1-x}Se_x$ [8-10], are practically linear and take into account the effects of the glass matrix pressure, phonon confinement, and surface phonon scattering [8], which are essential for Raman scattering in glass-embedded NCs. For $CdS_{1-x}Se_x$ NCs, Raman spectroscopy enables the chemical composition to be determined with the accuracy as high as $\Delta x = \pm 0.03$ [9]. However, one should hardly expect such an accuracy for $CdSe_{1-x}Te_x$ since in this ternary system the Raman frequencies are noticeably lower, resulting in much higher relative errors. Moreover, for NCs with high tellurium content, a rather small difference between the CdSe-like and CdTe-like LO phonon frequencies together with the Raman band broadening due to the phonon confinement and surface phonon contribution leads to an overlap of the CdSe-like and CdTe-like Raman bands, thus encumbering their resolution. Still, for $CdSe_{1-x}Te_x$ NCs, in particular for the range of compositions rather away from the end-point ones, Raman spectroscopy is a fast, reliable, and non-destructive technique to determine the average NC composition from the difference of the LO phonon frequencies. Fig. 2a shows the chemical composition of glass-embedded $CdSe_{1-x}Te_x$ NCs determined from the CdSe-like and CdTe-like LO phonon frequency difference in the measured Raman spectra using the known dependence built for the $CdSe_{1-x}Te_x$ system based on the Raman and infrared data available for bulk and nanoscale crystals [6].

Another Raman-based approach relies on the ratio of CdTe-like and CdSe-like LO phonon peak intensities. For ternary $CdS_{1-x}Se_x$ NCs, a correlation between the CdSe-like and CdS-like LO phonon band intensities and the S/Se ratio was reported and even used to quantify the chalcogen content in the NCs [9-12]. Still, the accuracy of this approach to determine the NC composition was admitted to be lower than that for the approach based on the LO phonon frequency difference [9, 10]. Even though for II-VI NCs the electron-phonon interaction is much lower than for the corresponding bulk materials [13], for the analysis of the CdSe-like and CdTe-like LO phonon intensities one should take into account the electron-phonon interaction factors (polaron constants) [10].

The resonance Raman scattering cross-section in a crystal is proportional to the electron-phonon coupling constant (polaron constant) α^* [14]:

$$\alpha_i^* = \left(\frac{1}{\varepsilon_\infty} - \frac{1}{\varepsilon_0}\right)\frac{2\pi e^2}{h}\left(\frac{m^*}{2h\omega_{LO}}\right)^{\frac{1}{2}}, \qquad (4.1)$$

where ε_0 and ε_∞ are the static and high-frequency dielectric permittivity values, e and m^* are the electron charge and effective mass, $h\omega_{LO}$ is the LO phonon energy. For two-mode ternary II-VI compounds, a model of two non-interacting oscillators implies additivity of their contributions to the Raman scattering cross-section. The polaron constants for CdTe and CdSe are 0.29 and 0.50, respectively [15]. The chemical composition of $CdTe_xSe_{1-x}$ NCs estimated from the integrated intensities of CdTe-like and CdSe-like LO phonon bands as $x_I = I_{LO1}/(I_{LO1} + I_{LO2})$ is plotted versus the composition for the same sample estimated from the LO phonon peak frequency difference in Fig. 2b without and with normalization by polaron constants. A better correlation is observed for the values obtained with the account of the polaron constants what is in agreement with the results known for $CdS_{1-x}Se_x$ NCs [10].

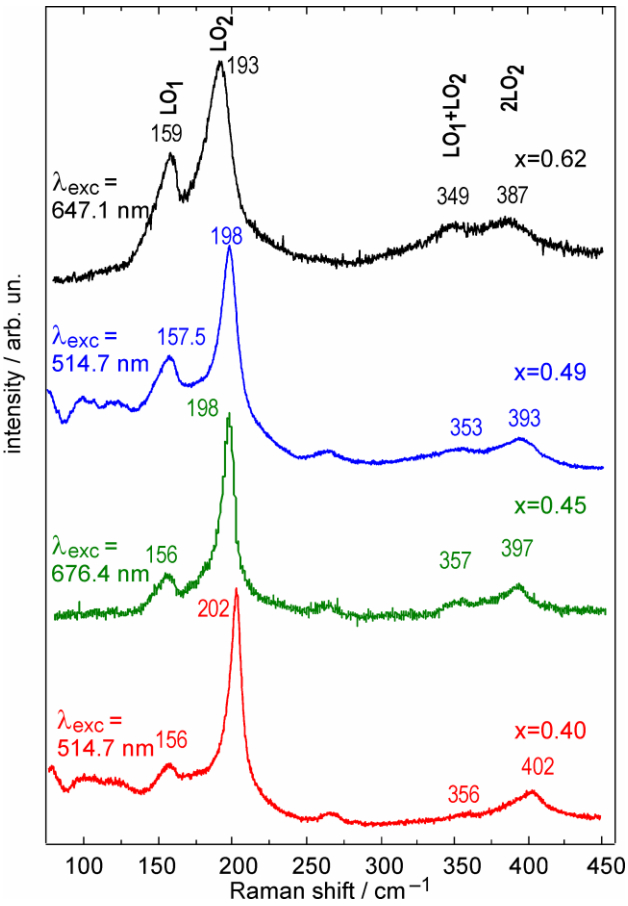

Fig. 1 – First- and second-order Raman spectra of $CdSe_{1-x}Te_x$ NCs embedded in borosilicate glass

In view of the possibilities to increase the accuracy of Raman-based approaches to fast, efficient, and non-destructive evaluation of the composition of matrix-embedded ternary NCs, it seems also important to check whether second-order Raman scattering data can be used for this purpose. As can be seen from Fig. 1, the Raman spectra of $CdSe_{1-x}Te_x$ NCs in borosilicate glass, apart from the CdTe-like LO_1 and CdSe-like LO_2 phonon bands and acoustic phonon density-of-states maxima near 100-120 cm^{-1} (the latter are revealed due to the confinement-related breakdown of the Raman selection rules and, additionally, due to compositional disorder), contain clear two-phonon maxima in the range 350-450 cm^{-1}. The intensities and widths of the $LO_1 + LO_2$ and $2LO_2$ maxima enable their spectral positions to be reliably determined with high accuracy. The linear dependence of the difference of the $2LO_2$ and $(LO_1 + LO_2)$ phonon peak frequencies in the Raman spectra of $CdSe_{1-x}Te_x$ NCs on their chemical composition determined from the first-order Raman spectra (Fig. 2c) shows the possibility of two-phonon Raman spectroscopy to be applied to determine the chemical

composition of NCs of this ternary system.

It should be noted that Raman scattering was also employed for the characterization of $CdSe_{1-x}Te_x$ NCs produced by high-energy ball milling [16] and colloidal synthesis [17, 18]. In the first two cases the LO phonon frequencies and the chemical composition are in good agreement with the dependence in Fig. 2a [16, 17]. Meanwhile, in a recent paper [18] for Ni-doped $CdSe_{0.5}Te_{0.5}$ NCs, the authors observed a single mode near 180 cm^{-1} (intermediate between the CdTe and CdSe LO phonon frequencies) in the Raman spectrum, which supposes a one-mode behavior, thereby contradicting the whole array of the known Raman and infrared data for $CdSe_{1-x}Te_x$ [4, 6, 16, 17, 19, 20 and references therein]. Such behavior can hardly be related to doping with small amounts of Ni and the issue of reasonable explanation of the data in Ref. [18] still remains open.

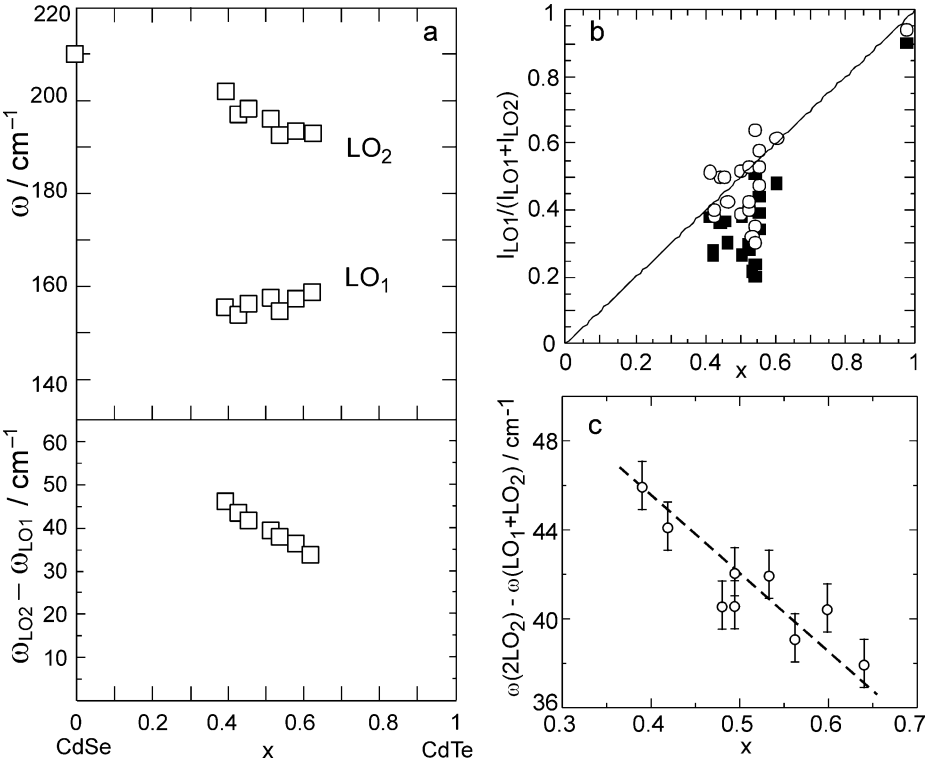

Fig. 2 – (a): Compositional dependence of CdSe-like and CdTe-like LO phonon frequencies and their difference in the Raman spectra of glass-embedded $CdSe_{1-x}Te_x$ NCs; (b): $CdSe_{1-x}Te_x$ NC composition determined from the CdSe-like and CdTe-like LO phonon band intensity ratio in the Raman spectra versus the composition determined from the CdSe-like and CdTe-like LO phonon frequency difference: solid squares – without correction, open circles – with correction for the polaron constant values; (c): $CdSe_{1-x}Te_x$ NC composition determined from the difference of the second-order $2LO_2$ and (LO_1 + LO_2) peak frequencies in the Raman spectra versus the composition determined from the CdSe-like and CdTe-like LO phonon frequency difference

We employed Raman spectroscopy to check how the thermal treatment conditions (temperature T_a and duration τ) affect the chemical composition of $CdSe_{1-x}Te_x$ NCs obtained in borosilicate glass by diffusion-limited growth. For the related $CdS_{1-x}Se_x$ NC system, this had been a long-debated issue until in our targeted study [3] it was shown that the behavior of the chalcogen content in the NCs under thermal treatment depends on the initial S/Se ratio. Namely, for sulfur-rich NCs the S content further increases with T_a and τ, for selenium-rich NCs the Se content increases, while for the samples with S/Se ratio close to 1 the NC composition remains independent of T_a and τ [3]. For $CdSe_{1-x}Te_x$, to our knowledge, no studies on the effect of thermal treatment parameters on the NC composition have been reported up to now.

Raman spectra of borosilicate glass samples with $CdSe_{1-x}Te_x$ NCs grown from the same initial mixture by thermal treatment at 625 °C at different durations are shown in Fig. 3. It can be seen that with increasing thermal treatment duration τ, CdTe-like and CdSe-like LO phonon peaks diverge, indicating a decreasing tellurium content x from 0.60 to 0.44. Such behavior was observed for different series of the samples prepared. This is drastically different from the diffusion-limited growth of $CdS_{1-x}Se_x$ NCs, for which a roughly similar chalcogen content in the initial mixture ($0.4 < x < 0.6$) is the same in the NCs at different thermal treatment parameters [3]. Most likely, this is related to the known ability of tellurium atoms to aggregate which can be revealed at longer thermal treatment and elevated temperatures, e.g., for samples with CdTe NCs grown in silicate glass, the Raman spectra provide evidence for Te_2 molecular dimers [19, 21]. The Raman features of elemental tellurium precipitated from CdTe single crystals [22] and films [23] were reported by different research groups. In our case, elemental tellurium is also formed in borosilicate glass samples doped with Cd, Se, and Te: the spectra of the sample subjected to thermal treatment at 700 °C for 12 h (the topmost curve in Fig. 3) reveal two intense peaks at 120 and 139 cm^{-1}. These peaks are known to corre-

spond to A_1 and E modes of elemental tellurium, respectively [22, 23]. Hence, one can assume that while at more intense and/or durable thermal treatment a part of Te atoms in the sample aggregates in extended Te precipitates, the tellurium content in the $CdSe_{1-x}Te_x$ NCs reasonably decreases as confirmed by the Raman spectra.

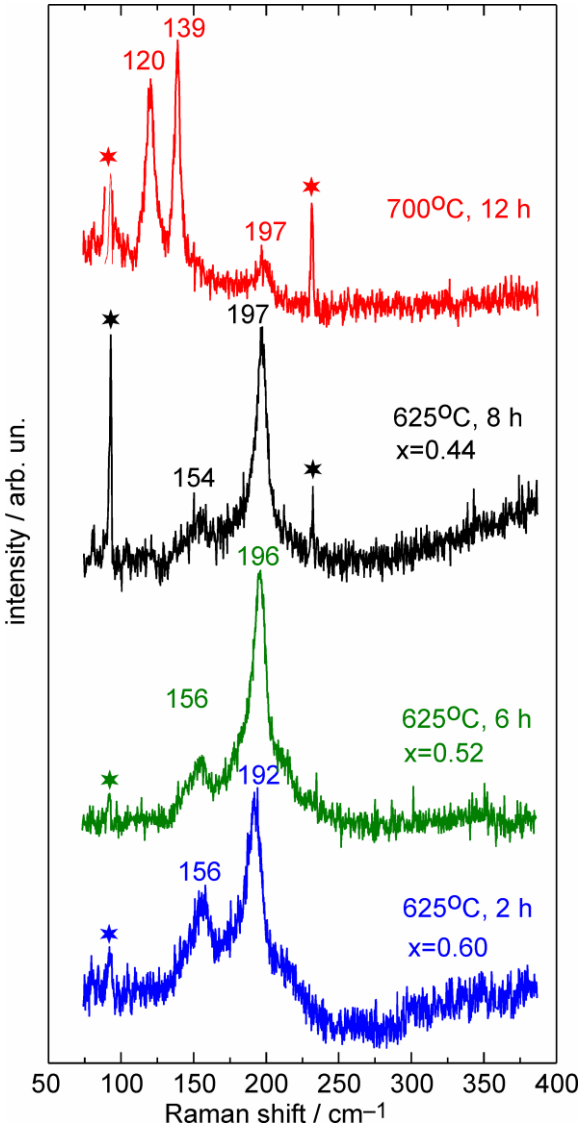

Fig. 3 – Raman spectra of borosilicate glass samples with $CdSe_{1-x}Te_x$ NCs grown from the same initial mixture by thermal treatment at 625 °C with different durations as well as the spectrum of a sample prepared from the same mixture at 700 °C (the topmost curve) with intense bands of elemental tellurium. The spectra were measured under 647.1 nm laser excitation at room temperature. Asterisks denote Kr^+ laser plasma peaks

Typical optical absorption and PL spectra of glass-embedded $CdSe_{1-x}Te_x$ NCs are shown in Fig. 4. Confinement-related maxima in the optical absorption spectra of glass-embedded $CdSe_{1-x}Te_x$ NCs enabled their average size to be estimated In the framework of the effective-mass approximation [24], while their smeared appearance revealed a noticeable size dispersion. The average NC size predictably increases with the thermal treatment duration and temperature.

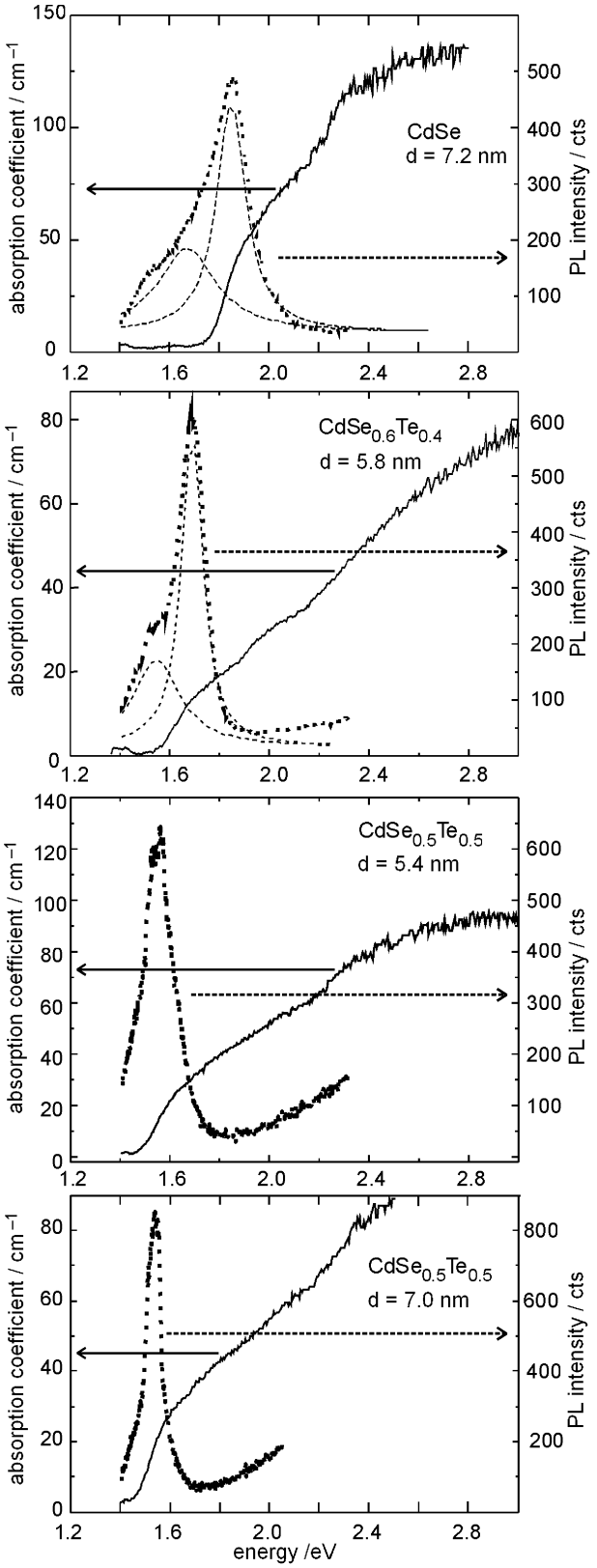

Fig. 4 – Optical absorption (solid curves) and PL (dots) spectra of borosilicate glass-embedded $CdSe_{1-x}Te_x$ NCs measured at room temperature. Short-dashed curves show the experimental PL data approximation by two Gaussian contours

It can be seen from Fig. 4 that the PL spectra of glass-embedded $CdSe_{1-x}Te_x$ NCs are dominated by a relatively narrow (0.1-0.2 eV) peak with a maximum

slightly below the first confinement-related maximum in the absorption spectra corresponding to the transition between the $1s_e$ conduction band state and the $1S_{3/2}$ valence band state (HOMO-LUMO) in NCs [25]. This PL maximum with energy close to the band gap is usually explained in the framework of the "dark exciton" model taking into account the exciton state fine structure arising due to structural anisotropy and electron-hole exchange interaction [26]. An alternative explanation, especially with regard to the PL bandwidth, is based on exciton scattering by acoustic phonons [27]. The Stokes shift (the energy difference between the first confinement-related absorption maximum and the near-edge PL peak), typically for II-VI NCs, decreases with the NC size down to 0.01-0.02 eV (Fig. 4). Evidently, for NCs grown in borosilicate glass the non-resonant component of the Stokes shift related to the NC size dispersion is predominant. The number of states in NCs, to which charge carriers can be excited by incoming light, the subsequent transition of the excited electrons and holes to the corresponding lowest-energy size-quantization levels and the radiative recombination from these levels are proportional to the NC volume while the total oscillator strength for the transition to these states is practically independent of the NC size [28, 29]. Meanwhile, the energy position of the first confinement-related maximum in the absorption spectrum is to a great extent determined by the NC size distribution and corresponds to the NCs of the average (predominant) size. This fact is actually responsible for the Stokes shift [29]. Resonant Stokes shift, explained by the existence of "dark" and "bright" excitons, energy-splitted by electron-hole exchange interaction [28], in this case plays a less prominent role.

A broader and weaker PL band, observed at lower energy as a shoulder for the samples with predominant selenium content, is usually related to recombination with the participation of surface states, including chalcogen traps or anion vacancies [27]. For the samples with higher Te content, it becomes less pronounced and practically vanishes. This observation is different from the case of glass-embedded $CdSe_{1-x}Se_x$ NCs where the surface-mediated PL is much more pronounced and often dominates in the PL spectra [30].

It is also worth mentioning that contrary to the $CdSe_{1-x}Se$, system, the compositional behavior of the $CdSe_{1-x}Te_x$ band gap is non-monotonous with a minimum near $x = 0.6$ [31]. Therefore, for $CdSe_{1-x}Te_x$ NCs with noticeable or predominant Te content the spectral positions of the PL maxima are much more affected by the NC size rather than their composition.

4. CONCLUSIONS

Borosilicate glass-embedded $CdSe_{1-x}Te_x$ NCs were prepared by diffusion-limited growth at a thermal treatment duration τ from 2 to 12 h and a temperature T_a from 600 to 700 °C. Optical absorption, photoluminescence (PL), and Raman spectroscopy were employed for the NC characterization. The NC chemical composition was determined based on the difference of CdSe-like and CdTe-like LO phonon frequencies in the Raman spectra. Alternative approaches to estimate the Se/Te ratio from the corresponding LO phonon peak intensities and from the second-order Raman spectra were analyzed. Based on the Raman data it was shown that for $CdSe_{1-x}Te_x$ NCs with roughly equal content of substitutive Se and Te atoms ($0.4 < x < 0.6$), the Te content slightly decreases with the thermal treatment temperature and duration. This is most likely related to elemental tellurium precipitation in the course of the thermal treatment.

Confinement-related maxima in the optical absorption spectra of glass-embedded $CdSe_{1-x}Te_x$ NCs enable their average size to be estimated, while their smeared appearance reveal a noticeable size dispersion. The PL spectra of glass-embedded $CdSe_{1-x}Te_x$ NCs are dominated by a rather narrow near band gap peak with a small Stokes shift, while a noticeably broader lower-energy surface-mediated PL band appears only as a shoulder and vanishes with increasing Te content. For $CdSe_{1-x}Te_x$ NCs with noticeable or predominant Te content, the PL maximum position is determined by the NC size rather than their composition in view of the non-monotonous compositional behavior of the $CdSe_{1-x}Te_x$ band gap.

ACKNOWLEDGEMENTS

Y.M. Azhniuk is grateful to Chemnitz University of Technology (Visiting Scholar Program) for the support of his research stay at the university.

REFERENCES

1. D.V. Talapin, J.-S. Lee, M.V. Kovalenko, E.V. Shevchenko, *Chem. Rev.* **110**, 389 (2010).
2. N.F. Borrelli, D. Hall, H. Holland, D. Smith, *J. Appl. Phys.* **61**, 5399 (1987).
3. Yu.M. Azhniuk, A.V. Gomonnai, Yu.I. Hutych, V.V. Lopushansky, M.V. Prymak, I.I. Turok, V.O. Yukhymchuk, D.R.T. Zahn, *J. Cryst. Growth* **312**, 1709 (2010).
4. V. Spagnolo, G. Scamarcio, M. Lugará, G.C. Righini, *Superlattice. Microst.* **16**, 51 (1994).
5. I.V. Bodnar, V.S. Gurin, A.P. Molochko, N.P. Solovey, P.V. Prokoshin, K.V. Yumashev, *Semiconductors* **36**, 298 (2002).
6. Yu.M. Azhniuk, Yu.I. Hutych, V.V. Lopushansky, L.A. Prots, A.V. Gomonnai, D.R.T. Zahn, *phys. status solidi c* **6**, 2064 (2009).
7. B.T. Spann, X. Xu, *Appl. Phys. Lett.* **105**, 083111 (2014).
8. V.M. Dzhagan, Yu.M. Azhniuk, A.G. Milekhin, D.R.T. Zahn, *J. Phys. D: Appl. Phys.* **51**, 503001 (2018).
9. A. Tu, P.D. Persans, *Appl. Phys. Lett.* **58**, 1506 (1991).
10. Yu.M. Azhniuk, Yu.I. Hutych, V.V. Lopushansky, M.V. Prymak, A.V. Gomonnai, D.R.T. Zahn, *J. Phys. Chem. Solids* **99**, 66 (2016).
11. G. Scamarcio, M. Lugarà, D. Manno, *Phys. Rev. B* **45**, 13792 (1992).
12. W.S.O. Rodden, C.N. Ironside, C.M. Sotomayor Torres, *Semicond. Sci. Technol.* **9**, 1839 (1994).
13. A.M. Yaremko, V.O. Yukhymchuk, V.M. Dzhagan, M.Ya. Valakh, J. Baran, H. Ratajczak, *J. Phys.: Conf. Ser.* **92**, 012061 (2007).
14. R. Zeyher, *Solid State Commun.* **16**, 49 (1975).
15. M.Ya. Valakh, A.P. Litvinchuk, *Sov. Phys. Solid State* **27**, 1176 (1985).

16. S. Li, G. Tan, J.B. Murowchick, C. Wisner, N. Leventis, T. Xia, X. Chen, Z. Peng, *J. Electron. Mater.* **42**, 3373 (2013).
17. L.X. Hung, P.T. Nga, N.N. Dat, N.T.T. Hien, *J. Electron. Mater.* **49**, 2568 (2020).
18. N.X. Ca, N.T. Hien, P.N. Loan, P.M. Tan, U.T.D. Thuy, T.L. Phan, Q.B. Nguyen, *J. Electron. Mater.* **48**, 2593 (2019).
19. Yu.M. Azhniuk, V.V. Lopushansky, Yu.I. Hutych, M.V. Prymak, A.V. Gomonnai, D.R.T. Zahn, *phys. status solidi b* **248**, 674 (2011).
20. D.N. Talwar, T.-R. Yang, Z.C. Feng, P. Becla, *Phys. Rev. B* **84**, 174203 (2011).
21. W. Li, W. Zhang, M. Xia, C. Liu, J. Wang, *J. Appl. Phys.* **121**, 183104 (2017).
22. P.M. Amirtharaj, F.H. Pollak, *Appl. Phys. Lett.* **45**, 789 (1984).
23. O.R. Ochoa, F.J. Witkowski III, C. Colajacomo, J.H. Simmons, B.G. Potter, *J. Mater. Sci. Lett.* **16**, 613 (1997).
24. S.V. Gaponenko, *Optical Properties of Semiconductor Nanocrystals* (Cambridge University Press: 1998).
25. H.H. von Grünberg, *Phys. Rev. B* **55**, 2293 (1997).
26. M. Nirmal, D.J. Norris, M. Kuno, M.G. Bawendi, Al.L. Efros, M. Rosen, *Phys. Rev. Lett.* **75**, 3728 (1995).
27. D. Valerini, A. Creti, M. Lomascolo, L. Manna, R. Cingolani, M. Anni, *Phys. Rev. B* **74**, 235409 (2005).
28. Al.L. Efros, M. Rosen, M. Kuno, M. Nirmal, D.J. Norris, M. Bawendi, *Phys. Rev. B* **54**, 4843 (1996).
29. I.M. Kupchak, D.V. Korbutyak, S.M. Kalytchuk, Yu.V. Kryuchenko, A. Chkrebtii, *J. Phys. Stud.* **14**, 2701 (2010) [in Ukrainian].
30. Yu.M. Azhniuk, V.V. Lopushansky, M.V. Prymak, K.P. Popovych, A.M. Solomon, A.V. Gomonnai, D.R.T. Zahn, *J. Nano- Electron. Phys.* **8** No 3, 03024 (2016).
31. Z.C. Feng, P. Becla, L.S. Kim, S. Perkowitz, Y.P. Feng, H.C. Poon, K.P. Williams, G.D. Pitt, *J. Cryst. Growth* **138**, 239 (1994).

Оптична діагностика нанокристалів $CdSe_{1-x}Te_x$, вирощених у боросилікатному склі

Ю.М. Ажнюк[1,2], О.В. Гомоннай[1,2], Ю.І. Гутич[1], В.В. Лопушанський[1], Д.Р.Т. Цан[3]

[1] *Інститут електронної фізики НАН України, вул. Університетська, 21, 88017 Ужгород, Україна*
[2] *Ужгородський національний університет, вул. Підгірна, 46, 88000 Ужгород, Україна*
[3] *Фізика напівпровідників, Кемніцький технічний університет, D-09107 Кемніц, Німеччина*

Нанокристали (НК) $CdSe_{1-x}Te_x$ отримано методом дифузійно обмеженого росту в боросилікатному склі і досліджено методами спектроскопії поглинання, фотолюмінесценції (ФЛ) і раманівського розсіювання світла. Проаналізовано кілька підходів до визначення хімічного складу НК за даними раманівської спектроскопії. На основі раманівських даних показано, що для НК $CdSe_{1-x}Te_x$ з проміжним x ($0.4 < x < 0.6$) вміст Te дещо понижується зі зростанням температури і тривалості термообробки. Квантово-розмірні максимуми у спектрах оптичного поглинання вкраплених у скло НК $CdSe_{1-x}Te_x$ дають змогу визначити їх середній розмір, а розмитий характер максимумів свідчить про помітну дисперсію розміру. У спектрах ФЛ вкраплених у скло НК $CdSe_{1-x}Te_x$ домінує досить вузький пік прикрайової ФЛ з малим стоксівським зміщенням. а більш низькоенергетична смуга ФЛ з участю поверхневих станів проявляється тільки у вигляді плеча і зникає зі зростанням вмісту Te.

Ключові слова: Нанокристали, Дифузійно-лімітований ріст, Фотолюмінесценція, Раманівська спектроскопія.